Luminescent Solar Concentrators Employing Phycobilisomes

By *Carlijn L. Mulder, Luke Theogarajan, Michael Currie, Jonathan K. Mapel, Marc A. Baldo,* Michael Vaughn, Paul Willard, Barry D. Bruce, Mark W. Moss, Clifford E. McLain,* and *John P. Morseman*

Solar concentrators can significantly reduce the use of expensive semiconductor materials in photovoltaic (PV) energy conversion. Luminescent solar concentrators (LSCs) are especially promising because they do not need to track the sun to obtain high optical concentration factors.[1–6] In this work, we demonstrate LSCs employing phycobilisomes, which are photosynthetic antenna complexes that concentrate excited states in red algae and cyanobacteria.[7,8] The phycobilisomes are cast in a solid-state matrix that preserves their internal Förster energy-transfer pathways and large wavelength shift between absorption and emission. Casting is a simple fabrication technique that also eliminates any need for expensive high-index glass or plastic. By comparing the performance of intact and partly decoupled complexes, we establish that energy transfer within intact phycobilisomes reduces LSC self-absorption losses by approximately $(48 \pm 5)\%$. These results suggest that phycobilisomes are a model for a new generation of cast LSCs with improved efficiency at high optical concentrations.

LSCs are nontracking concentrators that redirect solar radiation into simple slab waveguides (see Fig. 1a). Light incident on an LSC is absorbed by dyes, re-emitted into a guided mode in the slab, and finally collected by a PV cell mounted at the edge of the slab. The maximum optical concentration of an LSC is theoretically limited by the wavelength shift between absorption and emission in the dye.[9] Larger wavelength shifts reduce the re-absorption of radiation already emitted into the LSC waveguide,[10,11] and alleviate compounding losses if either the photoluminescence efficiency of the dye, η_{PL}, or the fraction of emitted light trapped in the waveguide, η_{trap}, is less than unity.

[*] Prof. M. A. Baldo, C. L. Mulder, Dr. L. Theogarajan, M. Currie, J. K. Mapel
Department of Electrical Engineering and Computer Science
Massachusetts Institute of Technology
77 Massachusetts Avenue, Cambridge, MA 02139 (USA)
E-mail: baldo@mit.edu
M. Vaughn, P. Willard, Prof. B. D. Bruce
Biochemistry, Cellular and Molecular Biology & Chemical and Biomolecular Engineering
University of Tennessee at Knoxville
125 Austin Peay Bldg., Knoxville, TN 37996 (USA)
M. W. Moss, C. E. McLain, J. P. Morseman
Columbia Biosciences Corporation
6440 Suite D Dobbin Road, Columbia, MD 21045 (USA)

DOI: 10.1002/adma.200900148

Recently, Förster energy transfer has been used to mimic a four-energy-level laser design and minimize re-absorption losses in LSCs.[12] The key is the introduction of a low concentration of molecules that accept excited states from the surrounding LSC material. The low density of acceptor molecules takes over the light-emission function of an LSC, shifting the emissive wavelength away from the peak of the LSC absorption. Energy is gathered by the acceptor molecules using Förster energy transfer.[13–15] The bulk of the LSC can then be classified as donor molecules, whose function is to absorb light and transfer the energy to the acceptors. To minimize re-absorption losses on the acceptor, we must maximize the donor to acceptor ratio. Consequently, we must pack as many donor molecules as possible within the energy-harvesting range of every acceptor molecule, typically just 3–5 nm.[13,14] There are two methods for controlling the intermolecular spacing: 1) Deposit the donor and acceptor molecules in a thin film ($\sim$1 μm) on a waveguide. This approach draws on organic-semiconductor-device technology, and the subsequent device is known as an organic solar concentrator (OSC).[12] The substrate has to be very transparent glass or plastic, and it must have a higher refractive index than the film to prevent optical trapping in the organic layer. 2) Employ aggregates of dyes where multiple donor molecules are positioned within the Förster radius of relatively few acceptors. This second approach is compatible with the traditional LSC structure, in which dyes are cast at low density within a polymer matrix. Casting LSCs eliminates any need for expensive high-index glass, motivating our work on Förster-coupled dye aggregates in the form of phycobilisomes.

The decoupled optical and electrical functions of LSCs and their attached solar cells, respectively, are analogous to the separate light collection and charge generation tasks in photosynthesis.[16] Indeed, photosynthesis employs various light-collection structures that may be used in LSCs. In this work, we report solution-based and solid-state LSCs that use phycobilisomes.[7,8] Phycobilisomes are large water-soluble pigment-protein complexes that function as light-harvesting devices in red algae and cyanobacteria. They are capable of absorbing light over a broad range of the visible spectrum and efficiently concentrating this captured energy at the photosynthetic reaction center. The main components of phycobilisomes are phycobiliproteins, which serve as scaffolding for covalently bound, linear tetrapyrrole chromophores called bilins.[17] The chromophores are arranged through self-assembly in cascading Förster-energy-transfer pathways that couple short-wavelength

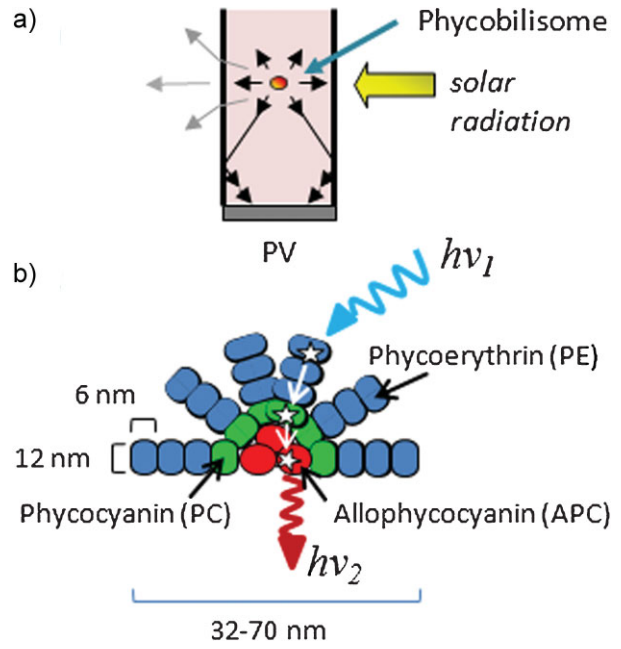

Figure 1. a) Schematic representation of an LSC. Solar radiation is absorbed by highly fluorescent dye molecules integrated in a thin, flat-plate waveguide. The dye re-emits photons at a lower energy, which can then be guided to the edge of the plate by total internal reflection to attached solar cells. b) Schematic representation of the structure of a phycobilisome, a macromolecular protein complex.[7] Hemispherically organized rods of PC and/or PE biliproteins join a core of APC biliproteins. Each biliprotein serves as a scaffold for its own characteristic chromophores. The bulk of the absorption takes place in the rods, while the unique nanostructure facilitates energy transfer towards the core of the complex, resulting in a large Stokes shift.

chromophores at the extremities of the complex to long-wavelength chromophores at the core of the complex. The phycobilisome core is composed of allophycocyanin (APC) (see Fig. 1b), containing approximately 72 chromophores (phycocyanobilin) that absorb at $\lambda_{max} = 650$ nm. Depending on the organism, 4–6 phycocyanin (PC) radial rods are attached to the core; each rod contains approximately 18 chromophores (phycocyanobilin) absorbing at $\lambda_{max} = 620$ nm. Finally, in some organisms, the PC rods are capped by additional rod structures containing phycoerythrin (PE) with approximately 34 chromophores (phycoerythrobilin or phycourobilin) that absorb at either $\lambda_{max} = 545$ or 490 nm. The quantum efficiency of energy transfer within the phycobilisome complex typically exceeds 95%.[18] But when decoupled, energy transfer is prevented, and the chromophores emit light. The photoluminescent (PL) efficiency varies between $\eta_{PL} = 98\%$ for PE, 51% for PC, and 68% for APC.[18]

The total number of bilins per phycobilisome is highly variable between different species and even within a species under different growth conditions.[19] A typical estimate for the ratio of chromophores in PE, PC, and APC is 408:108:72, i.e., the ratio of donor to acceptor molecules is approximately 6:1 in phycobilisomes. This is lower than the 30:1 ratio reported in ref. 12, but the high ratio given in ref. 12 was due to the high density of donors, which increased the refractive index of the film to $n = 1.7$ and possibly necessitated the use of a more expensive substrate.

To cast phycobilisomes in solid-state waveguides, they must be incorporated within a matrix that mimics the native aqueous environment, while simultaneously providing a rigid substrate. Polyacrylamide hydrogels satisfy both requirements.[20–22] To increase the rigidity of the matrix, we used a lower water content than is normally used in polyacrylamide films for gel electrophoresis. To decrease stress in the film, we added an extra monomer with bulky groups, *N*-isopropyl acrylamide (NIPAM), to the acrylamide monomer increasing steric repulsion between chains. We also decreased the ratio of the crosslinker, bisacrylamide, to yield a lower crosslinking density. Equal portions of a 40% (w/v) water-based solution of 37.5:1 acrylamide/bisacrylamide solution (Sigma-Aldrich) and a 40% (w/v) solution of NIPAM (Sigma-Aldrich) in deoinized water were mixed thoroughly using a mini-vortexer (VWR). To this solution, a freshly prepared solution of ammonium persulfate (Sigma-Aldrich) was added up to a concentration of 1% (w/v) and vigorously mixed. In a separate vial, dry phycobilisomes were rehydrated with 100 μL of 0.1 M phosphate buffer, and a 1 mL solution of the monomeric acrylamide solution was added to this solution. To accelerate the polymerization, 1.5 μL of *N,N′*-tetramethylethylene diamine (TEMED, Sigma-Aldrich) was added. After gentle mixing, the resultant solution was allowed to polymerize at room temperature in a mini-hybridization chamber (Electron Microscopy Sciences). This resulted in smooth, flexible, optically clear films with a refractive index of $n = 1.6$,[23] potentially compatible with polycarbonate substrates. The films were square with a length of $L = 22$ mm and a thickness of $t = 0.5$ mm (see Fig. 2a).

To enable characterization, the optically smooth phycobilisome film was supported on a glass slide. We did not observe the transmission of phycobilisome photoluminescence into the glass substrate, probably due to the presence of an air gap between the gel and glass. The integrity of phycobilisomes in the films was examined by comparing the absorption and fluorescence spectra of phycobilisomes in films and in phosphate buffer (see Fig. 2c). The film absorbed 70% of the incident light at the peak absorption wavelength of $\lambda = 545$ nm, and the emission was measured from the face of the sample. Both the emission spectra in the phosphate buffer and in the acrylamide film show strong emission from APC and almost complete quenching of PE emission at $\lambda_{max} = 572$ nm,[7] suggesting the internal energy-transfer path is largely preserved. In the absence of packaging, the gels dried out and lost their smooth morphology within several hours, increasing optical scattering losses and obscuring the observation of possible phycobilisome photodegradation. Thus, all characterization was performed immediately after fabrication.

The optical quantum efficiency (OQE), η_{edge}, defined as the fraction of incident photons that is emitted from the edges of the OSC substrates, was characterized within an integrating sphere (see Fig. 2b). Edge and facial LSC emission was discriminated by selectively blocking the edge emission with black tape and a black marker. The spectrally resolved OQE was compared to the absorption of complexes in phosphate buffer in Figure 2c. The OQE of the film as a function of excitation wavelength matches the absorption spectrum of phycobilisomes in their native environment, confirming that the optical properties of the

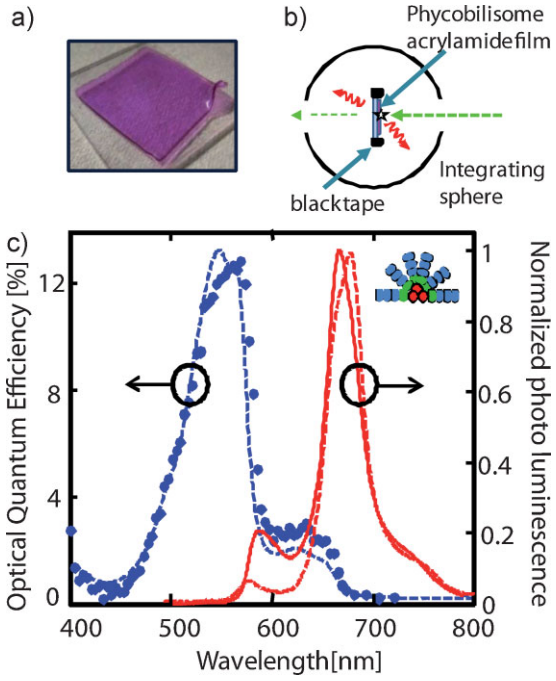

Figure 2. a) Photograph of a cast polyacrylamide film that contains intact phycobilisomes consisting of fully coupled PE, PC, and APC biliproteins. b) Schematic representation of the measurement set up used to determine the OQE of the phycobilisome film. The film ($n = 1.6$) was cast upon a high-index glass substrate ($n_S = 1.7$, Scott SF10 glass) and characterized in an integrating sphere to measure its edge emission as a function of excitation wavelength. c) OQE (blue dots) and normalized photoluminescence (red solid line) of the acrylamide phycobilisome (PE–PC–APC) films. The similarity of these data with the absorption and photoluminescence spectra of the phycobilisome complexes in phosphate buffer (dotted lines) demonstrates that the optical properties of the phycobilisomes are well preserved in the solid state film.

phycobilisomes are well preserved in the solid state. The peak OQE, $\eta_{edge} = 12.5\%$, compares well to the peak efficiencies exceeding $\eta_{edge} = 50\%$ in OSCs that use thin-film coatings of synthetic dyes.[12] The lower performance of cast phycobilisome-based LSCs was due to an absorption of only 70% of the incident light in the 0.5-mm-thick LSC at the peak absorption wavelength of 560 nm; the observation of a relatively low photoluminescent efficiency for APC in the films ($\eta_{PL} < 50\%$) and significant facial emission ($\eta_{face} = 12\%$) were probably due in part to scattering at the interface between the film and its glass substrate. This is consistent with optical reflection and transmission measurements of the gels, which yielded an upper limit of 3% per mm for the scattering loss in the glass bilayer. The low photoluminescent efficiency ($\eta_{PL} < 50\%$) relative to previous measurements[18] of APC ($\eta_{PL} = 68\%$) could be due to fact that it was incorporated into a solid state film.

Next, we examined the effect of near-field energy transfer on self-absorption losses within the phycobilisome-based LSCs. To eliminate any effects due to stress in the solid state films, we performed these measurements in aqueous LSCs, as shown schematically in Figure 3a. Sheets of glass (Erie Scientific, Portsmouth, 1 mm thick, $n = 1.5$) were cut and glued together with epoxy (Epo-Tek 301, Epoxy Technology, Billerica, MA) to form an aquarium with dimensions of 7.6 cm × 7.6 cm × 0.34 cm. A GaAs solar cell from Spectrolab (Sylmar, CA) with an external quantum efficiency (defined as electrons out per photon in) of ~90% was cut into 3.8 cm × 0.34 cm strips. Two of these cells were connected in series and attached to the edge of the concentrator with index-matching fluid (Norland Products, Cranbury, NJ). The other three edges were blackened out to prevent indirect luminescence reaching the solar cell. The phycobilisome solution was diluted in a 0.75 M phosphate buffer (pH 8.0) until the solution had an absorbance of 0.5 over a path length of 1 cm at the peak absorption wavelength. All liquid-based LSC measurements employed a mirror behind the LSC to add a second pass of pump radiation within the LSC.

The water-based LSCs employed three types of phycobilisomes: a stabilized, fully coupled phycobilisome with three types of biliproteins (PE–PC–APC), a partially coupled PC–APC complex, and a fully decoupled PC–APC complex. The stabilized phycobilisomes remained stable in solution up to one year at 4 °C.[24] The absorption and emission spectra of these phycobilisome complexes are shown in Figure 3b. The fully coupled complexes possessed an abundance of PE, leading to large Stokes shifts between the emission of APC at $\lambda = 680$ nm and the peak absorption of PE at $\lambda = 545$ nm. The partially coupled and fully decoupled complexes showed smaller Stokes shifts. The absorbance of the partially coupled and fully decoupled PC–APC phycobilisome complexes peaked at a wavelength of $\lambda = 620$ nm, where the PC protein has its peak absorption. The partially coupled PC–APC phycobilisomes showed no evidence of PC fluorescence at $\lambda = 650$ nm, suggesting full energy transfer to APC. For the decoupled complex, however, the observed emission was mostly due to decoupled PC chromophores that emit at $\lambda = 650$ nm.

The external quantum efficiency (EQE) as a function of geometric gain, G, for the liquid LSCs is presented in Figure 3c. G is defined as the ratio of the facial area to the area of the edges and is a key LSC parameter. It measures the path length of photons within the waveguide, and it determines the maximum possible optical concentration in the LSC. Typically, re-absorption losses increase with G.[12] The EQE was measured at $\lambda = 620$ nm for the partially coupled and fully decoupled complexes, and at $\lambda = 550$ nm for the fully coupled complexes containing PE. Consistent with the absorption and emission data, the Förster-coupled complexes were observed to have the best performance at higher geometric gain. The lower value of the EQE of the water-based LSCs compared to the OQE of the acrylamide films ($G = 11$) is due to a lower absorption coefficient, a lower trapping efficiency of the water-based system, loss due to coupling to the solar cell, and loss due to the non-unity EQE of the solar cell.

To quantitatively compare the different complexes, we defined the self-absorption loss as the decrease in EQE as a function of G relative to the EQE at $G = 1.4$. A direct comparison was easiest between the fully coupled and partially decoupled complexes because they both emit from APC. For all measured geometric gains, the intact phycobilisome complexes exhibited a self absorption loss that was (48 ± 5)% lower than the partially decoupled phycobilisomes. The fully decoupled complexes had the highest self-absorption losses of all due to the absence of

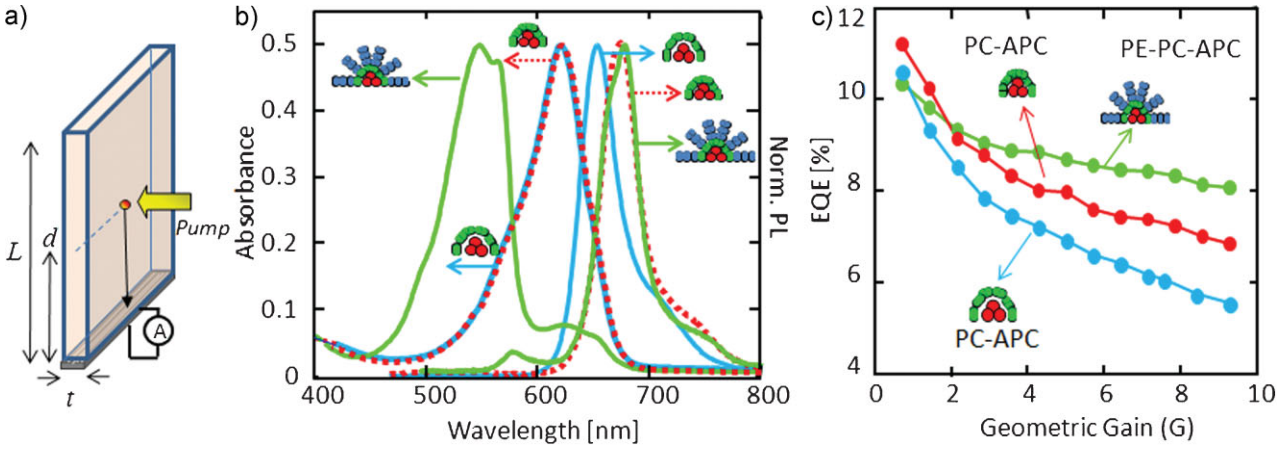

Figure 3. a) The performance of phycobilisome-based LSCs at higher optical concentrations was simulated by measuring the efficiency while varying the distance, *d*, between the excitation spot and the solar cell. b) Absorption and emission spectra of the phycobilisome complexes employed in the water-based LSCs. Green lines correspond to the fully coupled phycobilisome with three types of biliproteins (PE–PC–APC). The absorption of the partially coupled PC–APC complexes and fully decoupled PC–APC were identical (dashed red and solid blue line respectively). The emission spectrum of the decoupled complex is dominated by the PC emission (solid blue), while the emission of the partially coupled complex resulted from the APC bilins (dashed red line). The Stokes shift is largest for the fully coupled complex consisting of PE–PC–APC, while the decoupled complex has the largest overlap between absorption and emission spectrum. The self-absorption ratio, *S*, defined as the ratio between the peak absorption and the absorption at the peak emission wavelength[12] is 17.5, 10.1 and 1.7 for the fully coupled, partially coupled, and decoupled complexes respectively. c) External quantum efficiency versus geometric gain, *G*, of the water-based LSCs employing fully coupled PE–PC–APC phycobilisomes (green line), partially coupled PC–APC phycobilisomes (red line), and fully decoupled PC–APC phycobilisomes (blue line). The fully coupled complex has the best performance with geometric gain, reflecting its large Stokes shift, and hence reduced self-absorption losses.

energy transfer and subsequent emission by both PC and APC, resulting in a smaller Stokes shift.

To conclude, the unique self-assembled nanostructured phycobilisomes, which couple a large number of donor molecules to a handful of acceptors through an internal Förster energy pathway, reduced re-absorption losses in LSCs by approximately 50%. Thus, phycobilisomes provide a structural model for synthetic dyes in a new generation of cast LSCs with improved performance at high optical concentrations. We have also demonstrated that phycobilisomes themselves can be stabilized in a solid-state LSC matrix with minimal loss of performance. Future phycobilisome-based devices may be significantly improved by coupling efficient synthetic dyes to APC.[25] Additionally, the ratio of donor to acceptor pigments can be increased by selecting organisms with a better endogenous pigment ratio (either naturally occurring or through directed evolution).[26] Finally, the protein environment of the terminal pigment can be molecularly engineered to further improve the photostability and thermostability of phycobilisomes.[27]

Experimental

Optical characterization: All thin film absorption measurements were obtained using an Aquila spectrophotometer (Newport, Essek, UK). Spectrally resolved measurements employed a 150 W Xenon lamp coupled into a monochromator and chopped at 80 Hz for the OQE measurements and 20 Hz for the liquid-based LSCs. The photoluminescence for the OQE measurements was detected by a Si photodetector mounted directly on the integrating sphere. Fluorescence spectra of facial emission from LSCs were obtained using a 408 nm laser as an excitation source. *G*-dependent measurements were obtained by directing the excitation beam perpendicular to the LSC so as to create a spot of $\sim$1 mm^2, while the distance between the spot and the solar cell, *d*, was varied (Fig. 3a). The measured photocurrent was multiplied by the factor, *g*, that corrects for the different angle subtended by the solar cell at each spot distance: $g = \pi/tan^{-1}(L/2d)$, where *L* is the length of the edge of the LSC. This is an experimentally convenient technique to simulate the performance of LSCs at different geometric gains. It provides a lower bound for the performance because the average optical path-length is slightly longer than a uniformly illuminated LSC.

Phycobilisome Preparation: Intact phycobilisomes containing B-phycoerythrin (B-PE), R-phycocyanin (R-PC) and APC were isolated from the organism *Porphyridium Cruentum*. Cultures of *P. cruentum* were grown using a nutrient-supplemented media designed to replicate conditions in seawater, in a controlled-environment photobioreactor under low light ($<$1000$\times$) and high nitrate ($>$500 mg L^{-1}) conditions in order to induce a high level of phycobilisome production. Cultures were harvested after 4 weeks of growth by continuous flow centrifugation. The biomass was resuspended in 0.75 M potassium phosphate (pH 7.4, KPI) to maintain the appropriate ionic strength needed for intact phycobilisomes. The cells were disrupted by a microfluidizer, and cell wall debris and insoluble starches were removed by centrifugation. Intact phycobilisomes were then treated with a 1% (w/v) solution of detergent (Triton X-100, Sigma-Aldrich) in KPI buffer to solubilize and remove chlorophyll from the terminal emitter APC. After extraction of the chlorophyll, the phycobilisomes were precipitated by the addition of 20% (w/v) polyethylene glycol (PEG 8000, Sigma-Aldrich) followed by centrifugation at 4700 $\times$ *g* to pellet the phycobilisomes. The resulting pellet was resuspended overnight in 0.75 M KPI and purified by gel filtration column chromatography using CL-6B Sepharose resin (GE-HealthCare, Pittsburgh, PA). This step purified uncoupled phycobiliproteins, other cellular proteins, and protein aggregates as well as any residual chlorophyll away from the phycobilsomes. The purified phycobilisomes were then treated with 1% (v/v) formaldehyde overnight and quenched with 1% of a 1 M solution of lysine (pH 7.2, Sigma). The stabilized phycobilsomes were purified again over Sepharose CL-6B resin in 0.1 M sodium phosphate (pH 7.4) to remove any residual uncoupled phycobiliproteins and protein aggregates formed during the stabilization. The material was then freeze-dried in 0.1 M sodium phosphate (pH 7.4) with 0.2 M sucrose (Sigma-Aldrich). The non-PE

containing phycobilisome from Synechocystis PCC6803 were isolated using sucrose gradient centrifugation, as described in reference [17]. To study the effect of chromophore coupling on the LSC performance, unstabilized phycobilisomes were decoupled by diluting them in a 0.1 M phosphate buffer. At such low salt concentrations, the destabilized phycobilisomes decompose fully into their separate APC and PC proteins [28].

Acknowledgements

We thank DARPA, DOE, and NSF for financial support.

Received: January 14, 2009
Published online:

[1] W. H. Weber, J. Lambe, *Appl. Opt.* **1976**, *15*, 2299.
[2] A. Goetzberger, W. Greubel, *Appl. Phys.* **1977**, *14*, 123.
[3] a) J. C. Goldschmidt, M. Peters, P. Löper, O. Schultz, F. Dimroth, S. W. Glunz, A. Gombert, G. Willeke, in *Proc. 22nd Eur. Photovoltaic Sol. Energy Conf.* (Eds: G. Willeke, H. Ossenbrink, P. Helm) Wip-Renewable Energies, Munich, Germany, **2007**. b) J. C. Goldschmidt, M. Peters, A. Bösch, H. Helmers, F. Dimroth, S. W. Glunz, G. Willeke, *Sol. Energy Mater. Sol. Cells* **2009**, *93*, 176.
[4] V. Wittwer, W. Stahl, A. Goetzberger, *Sol. Energy Mater.* **1984**, *11*, 187.
[5] L. H. Slooff, E. E. Bende, A. R. Burgers, T. Budel, M. Pravettoni, R. P. Kenny, E. D. Dunlop, A. Büchtemann, *Phys. Status Solidi RRL* **2008**, *2*, 257.
[6] B. C. Rowan, L. R. Wilson, B. S. Richards, *IEEE J. Sel. Top. Quantum Electron.* **2008**, *14*, 1312.
[7] E. Gantt, *Annu. Rev. Plant Physiol. Plant Mol. Biol.* **1981**, *32*, 327.
[8] R. MacColl, *J. Struct. Biol.* **1998**, *124*, 311–334.
[9] G. Smestad, H. Ries, R. Winston, E. Yablonovitch, *Sol. Energy Mater.* **1990**, *21*, 99.
[10] J. S. Batchelder, A. H. Zewail, T. Cole, *Appl. Opt.* **1979**, *18*, 3090.
[11] J. S. Batchelder, A. H. Zewail, T. Cole, *Appl. Opt.* **1981**, *20*, 3733.
[12] M. J. Currie, J. K. Mapel, T. D. Heidel, S. Goffri, M. A. Baldo, *Science* **2008**, *321*, 226.
[13] T. Förster, *Discuss. Faraday Soc.* **1959**, *27*, 7.
[14] S. T. Bailey, G. E. Lokey, M. S. Hanes, J. D. M. Shearer, J. B. McLafferty, G. T. Beaumont, T. T. Baseler, J. M. Layhue, D. R. Broussard, Y.-Z. Zhang, B. P. Wittmershaus, *Sol. Energy Mater. Sol. Cells* **2007**, *91*, 67.
[15] B. A. Swartz, T. Cole, A. H. Zewail, *Opt. Lett.* **1977**, *1*, 73–75.
[16] R. E. Blankenship, *Molecular Mechanisms of Photosynthesis*, Wiley-Blackwell, Chichester, UK **2002**.
[17] A. N. Glazer, *Methods Enzymol.* **1988**, *167*, 291.
[18] J. Grabowski, E. Gantt, *Photochem. Photobiol.* **1978**, *28*, 47.
[19] R. MacColl, D. Guard-Friar, *Phycobiliproteins*, CRC Press, Boca Raton, FL, USA **1987**.
[20] R. P. Kennan, K. A. Richardson, J. H. Zhong, M. J. Maryanski, J. C. Gore, *J. Magn. Reson, Ser. B* **1996**, *110*, 267.
[21] R. M. Dickson, D. J. Norris, Y. L. Tzeng, W. E. Moerner, *Science* **1996**, *274*, 966.
[22] J. Franklin, Z. Y. Wang, *Chem. Mater.* **2002**, *14*, 4487.
[23] Y. M. Xu, I. Teraoka, *Macromolecules* **1999**, *32*, 4596.
[24] W. G. Telford, M. W. Moss, J. P. Morseman, F. C. Alnutt, *J. Immunol. Methods* **2001**, *254*, 13.
[25] Commercial products are available from Molecular Probes, Invitrogen, Eugene, OR.
[26] A. R. Grossman, M. R. Schaefer, G. G. Chiang, J. L. Collier, *Microbiol. Rev.* **1993**, *57*, 725.
[27] C. M. Toole, T. L. Plank, A. R. Grossman, L. A. Anderson, *Mol. Microbiol.* **1998**, *30*, 475.
[28] E. Gantt, C. A. Lipschultz, B. Zilinskas, *Biochim. Biophys. Acta* **1976**, *430*, 375.